Sensors and Materials, Vol. 11, No. 4 (1999) 247–256
MYU Tokyo

S & M 0369

The Strength of Surface Micromachined Indium Phosphide Devices Evaluated by Weibull Analysis of Tensile and Bending Tests

Staffan Greek, Christian Seassal*, Pierre Viktorovitch* and Klas Hjort

Department of Materials Science, Uppsala University, SE-751 21 Uppsala, Sweden
*LEAME-UMR CNRS 5512, Ecole Centrale de Lyon, 36 av Guy de Collongue, 69131 Ecully Cedex, Lyon, France

(Received November 2, 1998; accepted April 28, 1999)

Key words: tensile strength, bending strength, indium phosphide, Weibull statistics, reactive ion etch

The strength of beams surface micromachined from InP was evaluated by subjecting the beams to bending and tensile tests. The tests were performed with a testing unit mounted on a micromanipulator adapted for an SEM to facilitate *in situ* testing. The tests results were evaluated by Weibull analysis. Beams made from films deposited by identical processes were patterned with different reactive ion etching (RIE) processes and different mask materials. It was found that the etching process had a strong influence on the strength. Beams treated with a nondirectional RIE process, where much of the etching was due to chemical reactions, had a mean strength ($\bar{\sigma}$) of 1.9 GPa and a Weibull modulus (m) of 3.1 when evaluated with bending tests. Beams treated with a highly directional RIE process and the same mask material had $\bar{\sigma}$ of 1.3 GPa and m of 1.4. With a better mask material, the highly directional process produced beams with $\bar{\sigma}$ of 1.6 GPa and m of 2.8 when evaluated with bending tests. Tensile tests of beams on the same chips as the latter bending tests resulted in $\bar{\sigma} = 0.22$ GPa, $m = 3.4$. Comparing bending tests with tensile tests demonstrated that the tensile strength and the bending strength differ vastly. The Weibull parameters derived from fitting the Weibull probability function to the bending test data were used to predict the tensile strength, and the prediction was compared with the actual tensile test results.

1. Introduction

The mechanical strength is, for many reasons, an important parameter of surface micromachined devices. The devices should be able to withstand shock as well as long-term usage. At the same time, high-precision devices, *e.g.*, components for microoptoelectromechanical systems (MOEMS)[1,2], require that the design be made in such a way that the mechanical stress is optimized. In order to design devices optimally yet retaining an acceptable level of safety against fracture, methods to test and evaluate the strength of micromachined devices are necessary. Several testing methods are described in the literature, including the bending of cantilever beams[3] and uniaxial tensile tests of beams[4–6]. The results from bending and uniaxial tensile tests may seem conflicting unless they are subjected to Weibull analysis.

InP is the most suitable material for use in MOEMS for long optical wavelengths, *e.g.*, telecommunications. However, there is general skepticism concerning the mechanical strength of InP devices. Indeed, InP wafers are not as strong as wafers made from GaAs, and are much more fragile than silicon wafers. On the other hand, silicon is known to be an extremely strong material on a micromechanical level. Furthermore, GaAs-based devices were recently demonstrated to be much stronger than the strongest steel[7]. Therefore, the purpose of this study is to show that devices micromachined from InP possess sufficient strength for micromechanical applications.

It has been shown that the strength of silicon devices is governed by defects in the sidewalls[8]. In the case when reactive ion etching (RIE) is used to fabricate the devices, the surface characteristics (such as the defect density and severity) of the sidewall depend on the RIE process parameters as well as the mask material used. Strength testing is, in this case, a well-suited method to evaluate process improvement.

In this study, beams were surface micromachined from InP. Three batches of beams were manufactured using different etching conditions. The strength of the beams manufactured using two different RIE processes was measured from the bending tests. Weibull analysis was used to compare the results. The beams in one batch were evaluated by subjecting them to both bending and uniaxial tensile tests. The results from bending and tensile tests were compared using Weibull analysis. All tests were conducted in an SEM with a micromanipulator adapted for *in situ* testing.

2. Weibull Analysis

Like silicon and GaAs, InP is a brittle material. The characteristics of a brittle material are that it deforms only elastically until fracture, and that the strength of a device is determined by the largest stress-concentrating defect. Due to the rough surface and the small bulk of the test devices, a fracture crack is assumed to have originated from defects distributed over the surface area of the device. The strength of a typical surface micromachined device made from InP, therefore, depends both on the defect distribution and on the distribution of stress over the surface of the device. The fracture stress is a stochastic parameter that needs a statistical treatment. Weibull[9,10] has described a

probability function of the fracture events as

$$P_f = 1 - \exp\left\{-\int_A \left(\frac{\sigma_f - \sigma_u}{\sigma_0}\right)^m \mathrm{d}A\right\}, \tag{1}$$

where P_f is the probability that fracture occurs when a unit is exposed to stress σ_f, σ_u is the lowest limit at which fracture will occur, and σ_0 is a normalizing factor. The area A is the surface where cracks are initiated. The exponent m is a materials parameter known as the Weibull modulus, which expresses the statistical scatter of fracture events: a high Weibull modulus indicates a low scatter. Unless a large number of tests are performed to give a statistically significant value of the lowest fracture limit, σ_u is normally set to zero. In the case when fractures originate from defects within the device, *e.g.* from impurity precipitates, the integral in eq. (1) should be evaluated over the volume.

The stress distribution over the crack initiating surface differs between the case of uniaxial tensile stress and pure bending. Writing out eq. (1) explicitly in the case of a beam under uniaxial tensile stress gives the fracture probability

$$P_f = 1 - \exp\left\{-(2tL + 2bL)\left(\frac{\sigma_f}{\sigma_0}\right)^m\right\}, \tag{2}$$

where t is the thickness of the beam, b is the beam width and L is the beam length. When the fracture probability is known, the mean fracture strength of a uniaxially loaded beam can be calculated from

$$\bar{\sigma} = \frac{\sigma_0}{(2tL + 2bL)^{1/m}} \Gamma\left(1 + \frac{1}{m}\right), \tag{3}$$

where $\Gamma\left(1 + \frac{1}{m}\right)$ is the gamma function.

For a beam clamped at one end, with a bending force applied perpendicular to a vertical sidewall at the distance L from the clamp, the fracture probability is

$$P_f = 1 - \exp\left\{-\left(\frac{tL}{m+1} + \frac{bL}{(m+1)^2}\right)\left(\frac{\sigma_f}{\sigma_0}\right)^m\right\}, \tag{4}$$

and the mean fracture stress is

$$\bar{\sigma} = \frac{\sigma_0}{\left(\frac{tL}{m+1} + \frac{bL}{(m+1)^2}\right)^{1/m}} \Gamma\left(1+\frac{1}{m}\right). \quad (5)$$

3. Experiment

The test devices were released beams fixed to a support at one end and equipped with a ring at the other, as shown in Fig. 1. The purpose of the ring was to serve as a grip for the probe of a test unit during tensile tests. The beams were used for both tensile and bending tests. The beam length of the tensile test beams was about 420 μm, while the beams for bending tests were about 210 μm long. All the tested beams were 35 μm wide and 4 μm thick. The actual dimensions were measured in an SEM in each case. Concave corners were given radii of 10 μm to decrease the otherwise high stress concentration that occurs at sharp corners.

The test devices were made from a 4-μm-thick InP layer epitaxially grown by metal-organic chemical vapor deposition (MOCVD) onto a 1-μm-thick layer of lattice matched InGaAs. The InGaAs was later used as sacrificial layer, i.e. it was selectively etched away to make freely standing microbeams. A 200-nm-thick SiO_2 layer was used as mask material for dry etching. Two methods of deposition were used to form the mask layer. Mask1 was deposited by PECVD assisted by ECR at room temperature, while Mask2 was deposited by electron beam evaporation. The beams were patterned by optical microlithography and dry etching. Two etching processes were performed on a Nextral NE 110 reactive ion etcher equipped with standard mass flow controllers. The nondirectional etching process with pronounced chemical attack consisted of 1 h and 15 min of etching in a plasma of 25 sccm CH_4, 12.5 sccm H_2 and 12.5 sccm Ar at 70 mTorr and –225 V. The nondirectional process is denoted as RIE1 hereafter. The process with a higher degree of directionality and physical etching, denoted as RIE2, consisted of etching for 4 h of in a plasma of 9.2 sccm CH_4 and 30.8 sccm H_2 at 15 mTorr pressure and –600 V. Afterwards, sacrificial etching of the InGaAs layer was performed in order to fabricate free-standing and movable InP beams for the tensile and bending tests. This was easily performed with a HF : H_2O_2 : H_2O ; (1:1:10) etchant. This solution provided lateral underetching of InGaAs with complete selectivity with regard to InP and an etch rate of 0.8 μm/min. In order to free the widest beams, an etching time of 50 min was required. The beams were dried by either sublimation of *tert*-butyl alcohol[11] or critical point drying in CO_2.[12]

The tensile and bending tests were done using an equipment developed at Uppsala University for testing micromachined devices. The equipment consists of a test unit mounted on a micromanipulator, and the test setup fits into an SEM. The test unit has stiff probe fixed to a movable arm, in which the force can be continuously measured with a force sensor. Once the test devices are placed in the micromanipulator, all handling and testing can be performed ***in situ*** and viewed at high magnification at the same time. Tensile testing of surface micromachined silicon using this equipment is described in ref. 6, where further

details are given. The tensile test was done using the micromanipulator to position the probe of the test unit in the ring of the test beam (Fig. 1(a)). The test unit was then activated to perform a tensile test by increasing the uniaxial force in the beam until fracture. The tensile strength was taken as

$$\sigma_f = \frac{F}{tb}, \tag{6}$$

where F is the force at fracture. Bending tests were made by positioning the probe to a sidewall and increasing the force perpendicular to the sidewall until the beam fractured Fig.

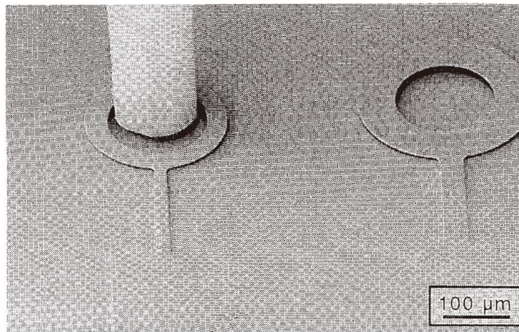

(a)

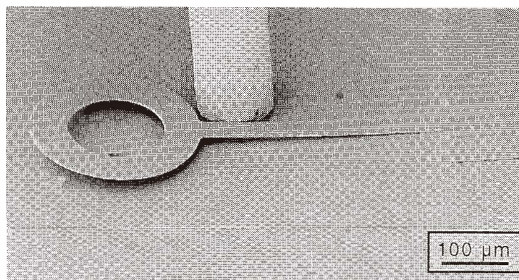

(b)

Fig. 1. (a) Beam of InP undergoing tensile test. The beam is fixed at one end. The probe of the test unit is seen at the top. (b) Bending test of an InP beam. The probe of the test unit exerts a bending force normal to the sidewall of the beam.

1(b). The bending force was applied 150 μm from the base of the beam. The bending strength was calculated from linear beam theory as

$$\sigma_f = \frac{6FL}{tb^2}. \tag{7}$$

The undeformed dimensions of the beam are used in both the tensile and bending strength formulas, i.e. the strength is the "engineering strength."

Bending tests were performed on beams made by RIE1 using Mask1, RIE2 using Mask1, as well as RIE2 using Mask2. Tensile tests were performed on beams made with RIE2 and Mask2.

4. Results

The fracture surfaces as investigated by SEM were clean and had no dimples or necking, indicating that the fracture was brittle, as expected. The fracture is caused by a sudden a catastrophic growth of one crack through the structure. The results are summarized in Table 1.

The devices etched out by RIE1 using Mask1 had nondirectionally etched sidewalls. When testing the smooth, but nonvertical RIE1-etched beams, a strong bending moment was introduced into the ring during tensile tests. This introduced a large bending stress to the ring and caused it to break before the beam fractured. When etching by RIE2 using Mask1, nonhomogeneous erosion of the mask resulted in a very rough sidewall. With the denser Mask2, a high selectivity is shown. Therefore, the vertical sidewalls created by the combination of RIE2 and Mask2 are nearly as smooth as those achieved by RIE1.

Figure 2 shows the strength of beams masked with Mask1 and etched by RIE1 and RIE2 processes. The Weibull fracture probability function of bending tests, eq. (4), was fitted by the chi-square method to the test data. The Weibull modulus and the mean

Table 1
The results obtained from strength testing. The Weibull modulus, m, the mean strength, $\bar{\sigma}$, and the fracture probability at 100 MPa, $P_f(100)$, are given in each case.

	Bending test				Tensile test			
	#Test	m	$\bar{\sigma}$ [Gpa]	$P_f(100)$	#Test	m	$\bar{\sigma}$ [Gpa]	$P_f(100)$
RIE1, Mask1	14	3.1	1.9	0.00007				
RIE2, Mask1	20	1.4	1.3	0.026				
RIE2, Mask2	27	2.8	1.6	0.0003	18	3.4	0.22	0.048

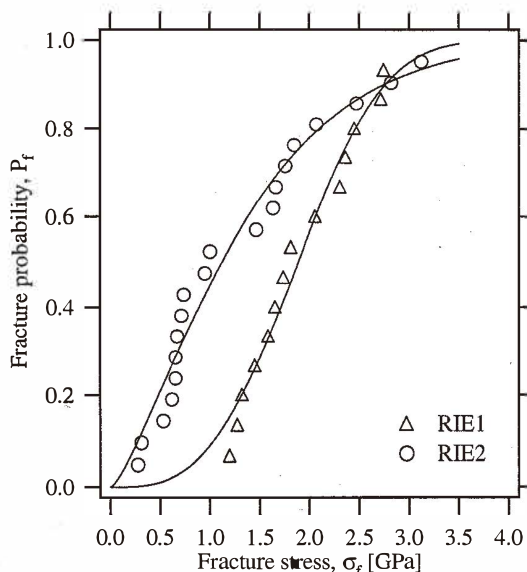

Fig. 2. Comparison between InP beams patterned by two different reactive ion etch processes, RIE1 and RIE2. In both cases, Mask1 was used as the mask material. The curves are the fitted Weibull probability functions.

fracture strength were derived from the fitted function. The scatter of test results is indicated by the Weibull modulus. RIE1 has a lower scatter of fracture values than RIE2. The mean stress of RIE1-etched beams is higher than that of RIE2-etched beams.

Figure 3 shows the results of bending tests together with those of tensile tests. The test beams were identically processed by RIE2 using Mask2. Bending test beams and tensile test beams were located close to each other on the processed chips. The Weibull probability function, eq. (2), was fitted to the tensile test data, while eq. (4) was fitted to the bending test data. The Weibull modulus and the mean fracture strength were derived from the fitted functions. The Weibull modulus is nearly the same in the two cases. The beams that were bent to fracture had a larger mean fracture strength than the beams with a uniaxial tensile load. The fitted parameters of the bending tests were input into eq. (2) to evaluate the ability to predict the tensile strength from bending tests. Predictions of tensile strength were also calculated on the assumption that the fractures originate from the sidewalls only, or from within the beam. This was done by evaluating eq. (1) over the sidewalls and the volume of the beams. The predictions were added to Fig. 3. Finally, the fracture probability at 100 MPa was calculated from the fitted function in each case and added to Table 1.

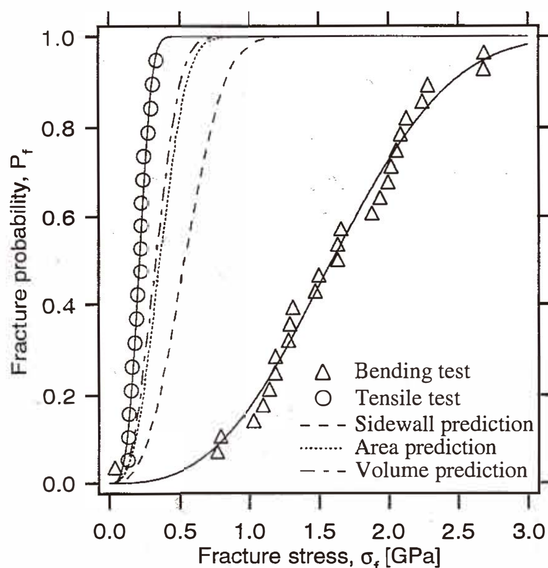

Fig. 3. Comparison between tensile and bending tests of InP beams. The beams were processed identically, by RIE1 using Mask2. The curves are the fitted Weibull probability functions. The results from bending tests are used to predict the tensile strength.

5. Discussion and Conclusions

The surface condition due to processing seems to be the most important factor affecting the fracture strength. Both RIE1 and RIE2 processes were used on identical InP material, but when Mask1 was used, RIE1 produced devices that were stronger and had a more even scatter of fracture-inducing defects. The scatter of defects is an important parameter when designing devices with specified reliability against fracture. This fact is demonstrated in Table 1 when comparing test beams manufactured by RIE2+Mask1 with test beams manufactured by RIE1. The RIE2 beams have a mean bending strength that is only 30% lower than the mean bending strength of RIE1 beams. However, the fracture probability at 100 MPa is for the RIE2 beams as high as 370% of that for the RIE1 beams, due to the lower Weibull modulus.

The result from bending tests can be used to predict the tensile strength by substituting the Weibull parameters m and σ_0 derived from the bending tests into the probability function of the tensile test device. Ultimately, the result from tests can be used to predict the strength of any device made by the same process steps, as long as the probability function is known, and the population of defects causing fracture is the same. Figure 3 shows that the bending tests tend to overestimate the tensile strength. This is explained by the fact that a larger portion of the tensile test beam than in the case of the bending test beam

is subjected to the testing stress. Therefore, there is a greater probability that rare defects initiate fracture during tensile tests than during bending tests. The accuracy of the different methods of prediction indicates that the fracture-initiating defects are scattered over the entire surface of the beams, or that volume defects cause the fracture. However, it seems improbable that there were volume defects severe enough to cause fracture at the low stresses of the tensile strength, given that the surface of a micromachined device is very large compared to the volume. On the other hand, the assumption that the fracture cracks originate from the sidewalls alone does not give an equally accurate prediction of the fracture probability (cf. Fig. 3). However, the SEM survey reveals no visible defects on surfaces other than the sidewalls. Our suggestion is that sidewall defects are the cause of the fractures at low stresses, especially in the tensile mode, but that defects from other populations (*e.g.*, top and bottom surface defects or volume defects) also cause fractures at higher stresses. To establish the nature of the defects causing fracture, it is suggested that beams of more varied dimensions be tested in larger quantities.

Stress concentration effect at the concave corner in the joint between the beam and the base has been omitted in the analysis. This well-known effect of stress concentration[13] increases the local stress at the fastening point of the beam compared with the stress calculated from linear beam theory. However, the stress concentration is a local phenomenon while the Weibull fracture theory concerns the total stress distribution integrated over the whole beam. Hence, the error made when assuming that the stress distribution conforms with linear beam theory over the whole test device is judged to be negligible.

The nondirectional RIE1 etch produced sidewalls in devices that were nonvertical. The highly directional RIE2 etch produced the desired vertical sidewalls in devices, but strength testing showed it to be inferior to RIE1 etched devices when a PECVD-deposited SiO_2 was used (Fig. 2). The solution to obtaining strong devices with vertical sidewalls was to use RIE2 with a mask material of higher quality, i.e., electron-beam-vaporized SiO_2 instead of PECVD-deposited SiO_2.

The reliability of InP as a material for surface micromachined devices is indicated by the fracture probability at 100 MPa (Table 1). The reason for the high fracture probability of devices under uniaxial tensile load is that the full beam is subjected to maximum stress. For typical MOEMS applications, maximum bending stresses of several tens of MPa can be foreseen. The fracture probability at 100 MPa is therefore relevant to use when comparing strengths. The fracture probability in the bending mode of beams with smooth sidewalls (processed by RIE1+Mask1 or RIE2+Mask2) is acceptable for most applications. Though the InP-based surface micromachined devices presented here have by no means optimized surface conditions, we have shown bending strengths much higher than that of the strongest steel. It is possible to improve the strength of InP. The surface conditions due to processing seem to be the most significant factor for the low fracture strength. Therefore, we are confident that we can develop stronger structures in the near future.

Acknowledgements

This work was financed by the ESPRIT project no. 22687 MOEMS. Donato Paquariello's help in CO_2 drying is greatly appreciated. The group of Professor Yves Monteil, at LMI, Universite Claude Bernard Lyon I, is gratefully acknowledged for providing the MOCVD epitaxial structure.

References

1 N. Chitica *et al.*: Physica Scripta (1998) in press.
2 S. Greek, R. Gupta and K. Hjort: J. Microelectromech. Syst. (1998) submitted.
3 S. Johansson, J.-Å. Schweitz, L. Tenerz and J. Tirén: J. Appl. Phys. **10** (1988) 4799.
4 J. Koskinen, J. E. Steinwall, R. Soave and H.H. Johnson: J. Micromech. Microeng. **3** (1993) 13.
5 W. N. Sharpe, B. Yuan, R. Vaidyanathan and R. L. Edwards: Proc. SPIE vol. 2880 (SPIE, Bellingham, CA, 1996) 78.
6 S. Greek, F. Ericson, S. Johansson and J.-Å. Schweitz: Thin Solid Films **292** (1997) 247.
7 K. Hjort, F. Ericson and J.-Å. Schweitz: Sensors and Materials **6** (1994) 359.
8 T. Tsuchiya, O. Tabata, J. Sakata and Y. Taga: J. Microelectromech. Syst. **1** (1998) 106.
9 W. Weibull: Roy. Swed. Soc. Eng. Proc. **151** (1939).
10 D. G. S. Davies: The Statistical Approach to Engineering Design in Ceramics in Proceedings of the British Ceramic Society, ed. D. J. Godfrey **22** (British Ceramic Society, Stoke-on-Trent, 1973) 429.
11 N. Takeshima et al.: Techn. Digest of the 6th International Conf. on Solid-State Sensors and Actuators, Transducers '91 (June 24–27, 1991, San Francisco, CA, USA) 63.
12 G. T. Mulhern, D. S. Soane and R. T. Howe: Techn. Digest of the 7th International Conf. on Solid-State Sensors and Actuators, Transducers '93 (June 7–10, 1993, Yokohama, Japan) 296.
13 S. P. Timoshenko and J. N. Goodier: Theory of Elasticity (McGraw-Hill, Singapore, 3rd ed. 1970) Chap. 50.